Jamming detection using geometric signatures in weather radar images

Dominique Faure[1], Pierre Tabary[1], Nicolas Gaussiat[1], Maud Martet[1]

[1] *METEO-FRANCE, 42, avenue Gustave Coriolis, 31057 Toulouse Cedex, France*

(Dated: 17 July 2014)

1 Context

Jamming is an increasing phenomenon in weather radar images. It usually affects specific directions, but has effects varying in time, figure and intensity (figure 1).

Météo-France has developed an automatic jamming detection procedure in order to produce statistics on jammed directions, and provide these statistics to the Agency in charge to identify the most important jamming sources. A first method has been implemented using values of a parameter describing the pulse-to-pulse fluctuation of the instantaneous return power from the same range gate. This procedure, currently routinely used for all radars of the French radar network, cannot be used for other radars which do not produce this parameter.

The method described in this communication is completely different. The method uses several algorithms to search and detect specific geometric signatures characterising jammed radar rays in a single polar radar image: three different algorithms for three types of signatures. This detection does not use quantitative values of radar returns, but only a binary coding of the pixels values (i.e. 1 = return / 0 = no return). In consequence these algorithms could be used with reflectivity images, rain rate images, or other parameters, and for any value of jammed pixels. This method may constitute a complementary (and independent) approach of other techniques using analysis of quantitative values of radar data.

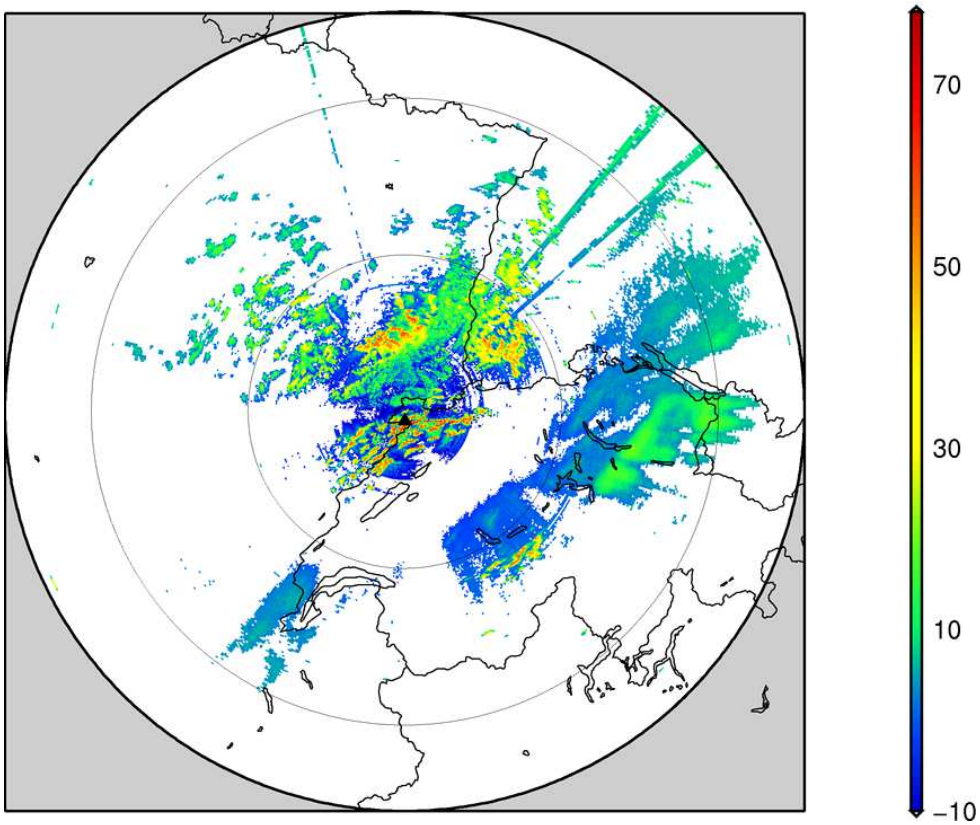

Figure 1: Example of radar image with jamming: Montancy radar at the frontier between France and Switzerland. Image size = 512x512km². Beam elevation = 0.4°. Scale = Reflectivity (dBZ). Date = 16 February 2014, 9h25 TU.

2 Method

Polar radar images are constituted of a series of rays for azimuths varying from 0° to 360°, each ray being constituted of a succession of range bins for range varying from 0 to the maximal range for radar measurement. Figure 2 presents such an image in Cartesian presentation (horizontal axis for azimuths, vertical axis for bins), named below *Im(az,bin)*.

In this picture, we can observe three kinds of geometric features, corresponding to three types of jamming signatures that the method searches to detect (figure 3). For each type of signature, a specific algorithm has been defined, using uniquely binary data: *Im(az,bin)* = 1 or 0 depending on whether it's value is above zero or not. For each algorithm, the jamming detection has two steps:

- step 1: estimating for each ray one or two selective indicators, whose values dramatically increase for rays affected by jamming
- step 2: analysing fluctuation of the indicators values on a series of rays in order to detect jammed rays, by trying to take into account the angular continuity of each signature and to define the angular limits of the jammed sectors.

For noisy images, we use a preliminary very simple filtering for each ray in order to eliminate isolated values above or equal to zero:

- *if (Im(az,bin)* > 0 *and Im(az,bin*-1*)* = 0 *and Im(az,bin*+1*)* = 0*) then Im(az,bin)* = 0
- *if (Im(az,bin)* = 0 *and Im(az,bin*-1*)* > 0 *and Im(az,bin*+1*)* > 0*) then Im(az,bin)* = 1

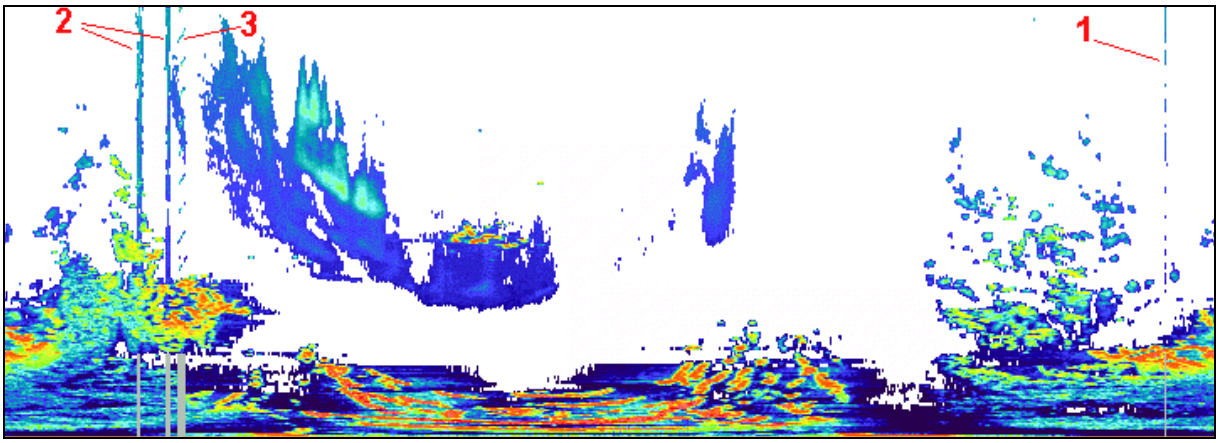

Figure 2: Polar image in Cartesian presentation (same image as figure 1): 720 rays in horizontal axis for azimuths, 256 bins in vertical axis (range-resolution = 1km). We can see 3 kinds of geometric features corresponding to 3 types of jamming signatures. The grey bars at the bottom represent the jamming signalisation produced by the algorithms presented in this communication.

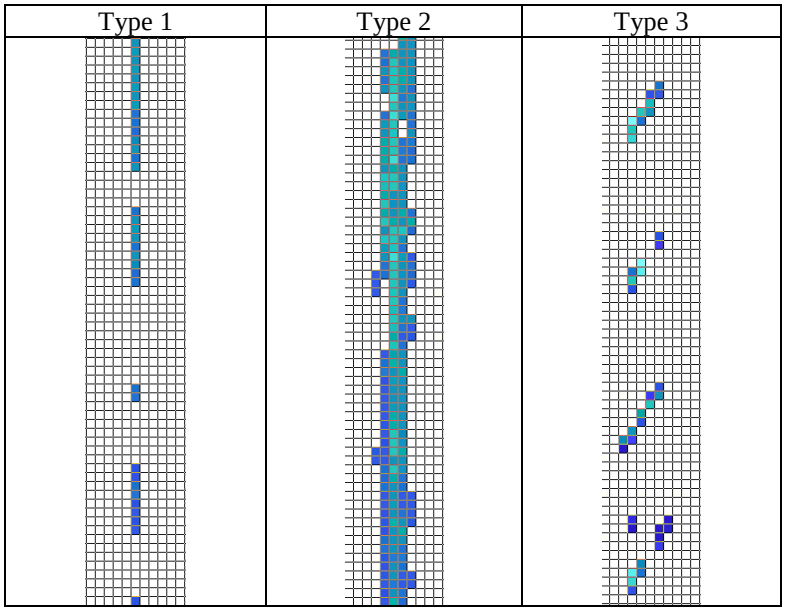

Figure 3: Detail of the 3 types of jamming signatures: Left, several continuous segments corresponding to the first type of signature. Middle, feature corresponding to the second type of signature, and an example of the third type of signature on the right.

2.1 Step1: Estimation of jamming indicators by ray

2.1.1 First type of signature

For this first type of signature, in Cartesian polar images the algorithm searches for continuous segments of rays corresponding to one (case 1) or two (case 2) successive rays having values above zero and surrounded by zero values. This means to search, for each bin along each *Im(az)* ray, the following binary feature along az-axis:

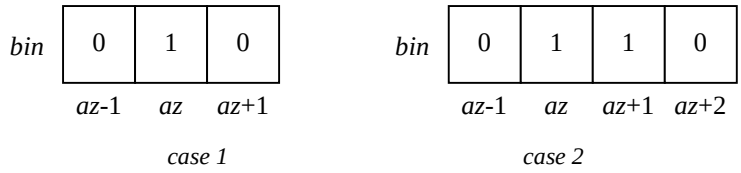

The algorithm estimates the length of each identified segment, and calculates the value of two indicators by *az* ray, for example for case 1:

- *S1(az)* = total number of bins corresponding to the feature for the entire ray
- *ST1(az)* = cumulated length of all segments having a segment-length above a threshold *T0*

and respectively, *S2* and *ST2* for case 2. In the results presented in this communication, threshold *T0* = 4.

2.1.2 Second type of signature

For the second type of signature, the principle of the algorithm is the same, but adapted to larger and irregular figures, in varying the angular distance *i* and *j* between the azimuth *az* of reference and the neighbouring *az-i az+j* azimuths, searching the following binary feature along az-axis:

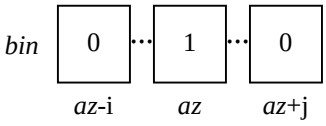

For each *az* ray, for a given couple of *(i,j)* values, the algorithm estimates the length of each identified segment and defines the value of one intermediate criterion *st3(az)*, and a threshold *T3(az)* increasing with *i* and *j* values:

- *st3(az)* = cumulated length of all segments having a segment-length above a threshold *T2*
- $T3(az) = C3 + 8(i+j-3)$ with *C3* a constant.

The algorithm determines the value of a first indicator by *az* ray:

- *ST3(az)* = maximal value of *st3(az)* found when *i* varies iteratively from 1 to *imax*, and *j* varies from 3 to *jmax*.

The iterative search for the concerned *az* ray is ended when *ST3(az)* > *T3(az)* or when *(i,j) = (imax,jmax)*, and the corresponding *(i-1)* and *(j-1)* values are saved for the final step as *iend(az)* and *jend(az)* limits. The condition $j > 2$ allows to avoid to treat again the first type of signature with a less appropriate algorithm. In the results presented in this communication, *imax* = 2, *jmax* = 6, *T2* = 8, and *C3* = 25.

2.1.3 Third type of signature

For this type of signature, the algorithm uses 4x6 matrixes of binary "masks" (figure 4), each matrix defining a form of signature to which image samples of 4x6 pixels are compared. The algorithm iteratively compares several binary masks to each binary sample of the *Im(az,bin)* image, by incrementing the reference bin of the sample along each *Im(az)* ray, in order to count the number *N4(az)* of complete equality between the two kinds of matrixes (masks and image samples).

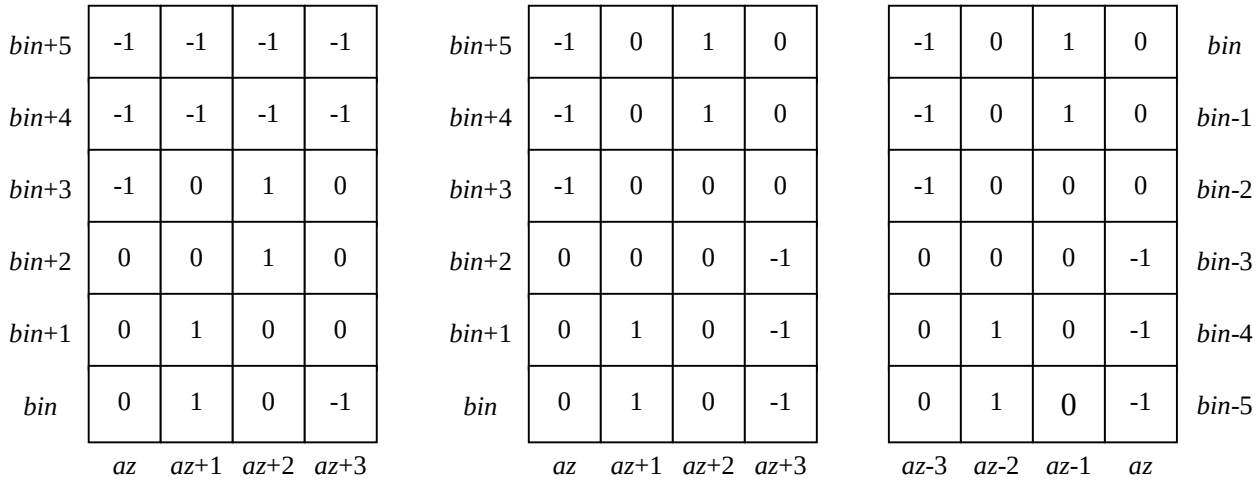

Figure 4: Example of 4x6 matrixes of binary masks: indexes corresponding to -1 values are not taken into account in the comparison with Im(az,bin) images. For each az azimuth, the reference bin for the comparison with image samples is named "bin".

The number and the features of the masks matrixes have to be adapted to the geometric signatures characterising jammed rays. In the results presented in this communication, 2 x 6 symmetric matrixes have been used.

2.2 Step 2: Indicators analysis and jamming signalisation

For the first type of signature, variation of *S1* and *ST1* values for case 1 allows to directly identify rays potentially jammed, and respectively *S2* and *ST2* for case 2 (figure 5).

For the second and third types of signature, who have angular continuity, a final step allows to integrate the first indicators on few rays in order to produce final indicators enhancing the angular continuity of the signature.

For the second type of signature, the final step integrates *ST3* and *T3* values on several rays defined by the *iend(az)* and *jend(az)* limits, in order to produce two another indicators named *SE3* and *TE3*. For all *az* rays, *SE3* equals *ST3* and *TE3* equals *T3*, except when *ST3* > *T3*. In this case, *T3* and *ST3* values are integrated as below:

- *TE3(az) = min(T3(k))* , *k* varying from *az-iend(az)* to *az+jend(az)*
- *SE3(az) = max(ST3(k))* , *k* varying from *az-iend(az)* to *az+jend(az)*

To not widen the result of the first type identification, a supplementary condition imposes *SE3(az)* = 0 if the concerned *az* ray has already been detected for the first type of signature and if *ST3(az)* = 0 and *iend(az)+jend(az)* ≤ 3. Finally, in order to avoid gaps in *SE3* detection the isolated zero values are filtered:

- *if (SE3(az)* = 0 *and SE3(az*-1*)* > 0 *and SE3(az*+1*)* > 0*) then SE3(az) = Moy(SE3(az*-1*),SE3(az*+1*))*

Variations of *SE3* and *TE3* values allow to identify rays potentially jammed (figure 5).

For the third type of signature, the *N4(az)* values are integrated over neighbouring rays having *N4* values above zero, from *az-ii* to *az+jj* rays, *ii* and *jj* varying from 0 to *ijmax* = 5 depending on the existence of *N4(az-ii)* or *N4(az+jj)* values above zero. This step allows to estimate three intermediate criterions:

- *NbN4(az)* = number of *N4* values above zero from *az-ii* to *az+jj*
- *SumN4(az)* = sum of *N4* values from *az-ii* to *az+jj*
- *MaxN4(az)* = maximal value of *N4* values from *az-ii* to *az+jj*

Finally, two indicators by *az* ray are produced, to highlight the angular continuity of the signature:

- *SE4 = SumN4(az)* if *MaxN4(az) > T4*, else *SE4 = N4(az)* with *T4* a constant threshold
- *NE4 = NbN4(az)* i*f MaxN4(az) > T4*, else *NE4* = 1

In the results presented in this communication, *T4* = 6.

Figure 5 shows the evolution with azimuth of the value of the final indicators *S1*, *ST1*, *S2*, *ST2*, *SE3*, *TE3*, *SE4*, *NE4*, for the Montancy radar image at 0.4° elevation, the 16 February 2014, 9h25 TU. These values are compared to several final thresholds (*FTn*), and a jamming signalisation is produced (figure 6) for azimuths having at least one of the following conditions true:

- *S1 > FT1* (*FT1* = 25),
- *ST1 > FT2* (*FT2* = 19),
- *S2 > FT1*,
- *ST2 > FT2*, (2.1)
- *SE3 > TE3*,
- *SE4 > FT3* (*FT3* = 12),
- *NE4 > FT4* (*FT4* = 4).

In summary, the algorithm used to detect the first type of signature (cases 1 and 2) requires three threshold values: *T0*, *FT1*, *FT2*. The algorithm used to detect the second type of signature necessitates one threshold value T2 and three parameters: *C3*, *imax*, *jmax*. The algorithm used to detect the third type of signature needs the definition of adapted binary mask matrixes, one parameter *ijmax*, and three threshold values: T4, *FT3*, *FT4*.

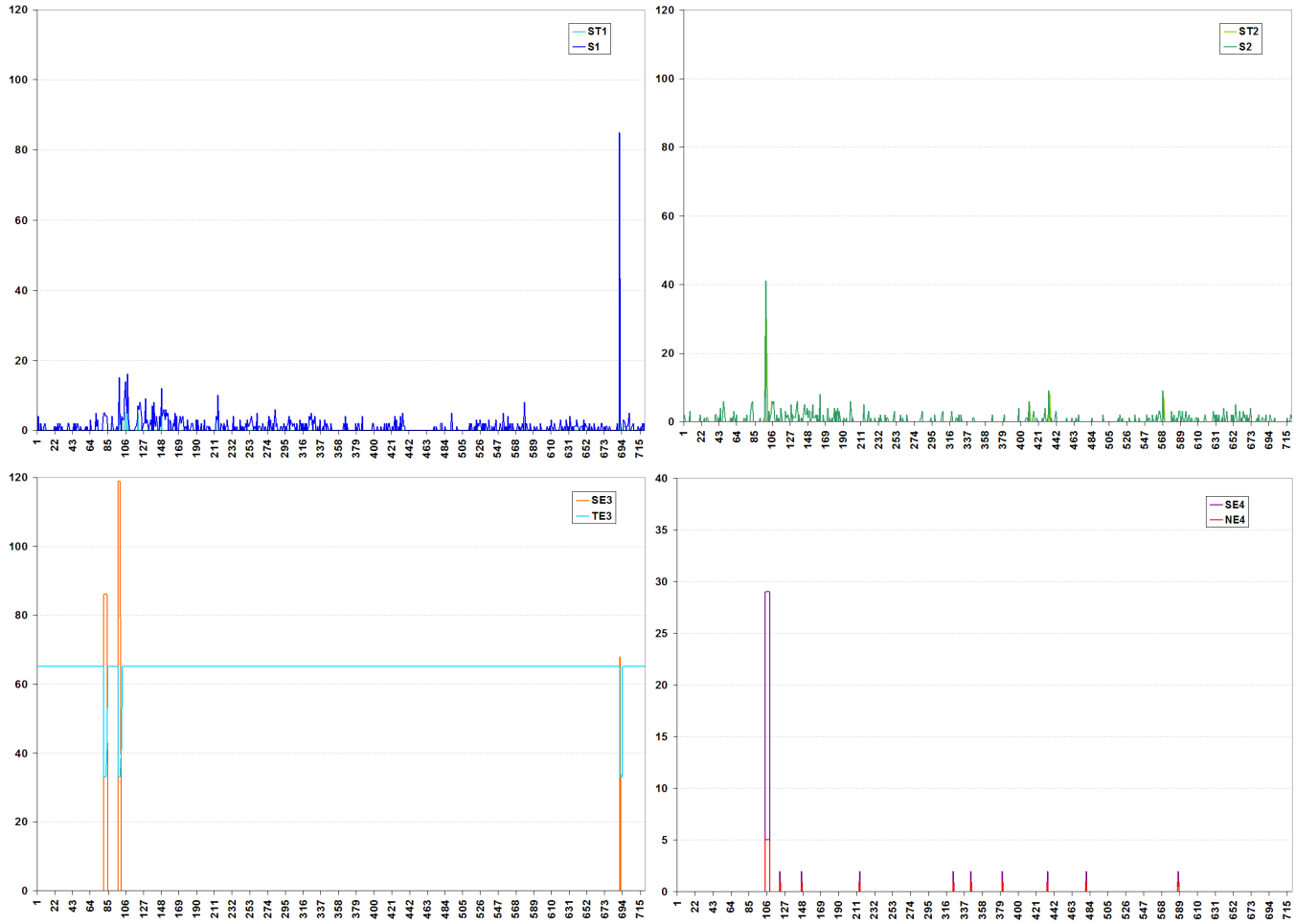

Figure 5: Evolution with azimuth of the S1, ST1, S2, ST2, SE3, TE3, SE4, NE4 values, for the Montancy radar image at 0.4° elevation, the 16 February 2014, 9h25 TU. This image shows one type 1 signature (case 1), two type 2 signatures, one type 3 signature (cf. figure 2).

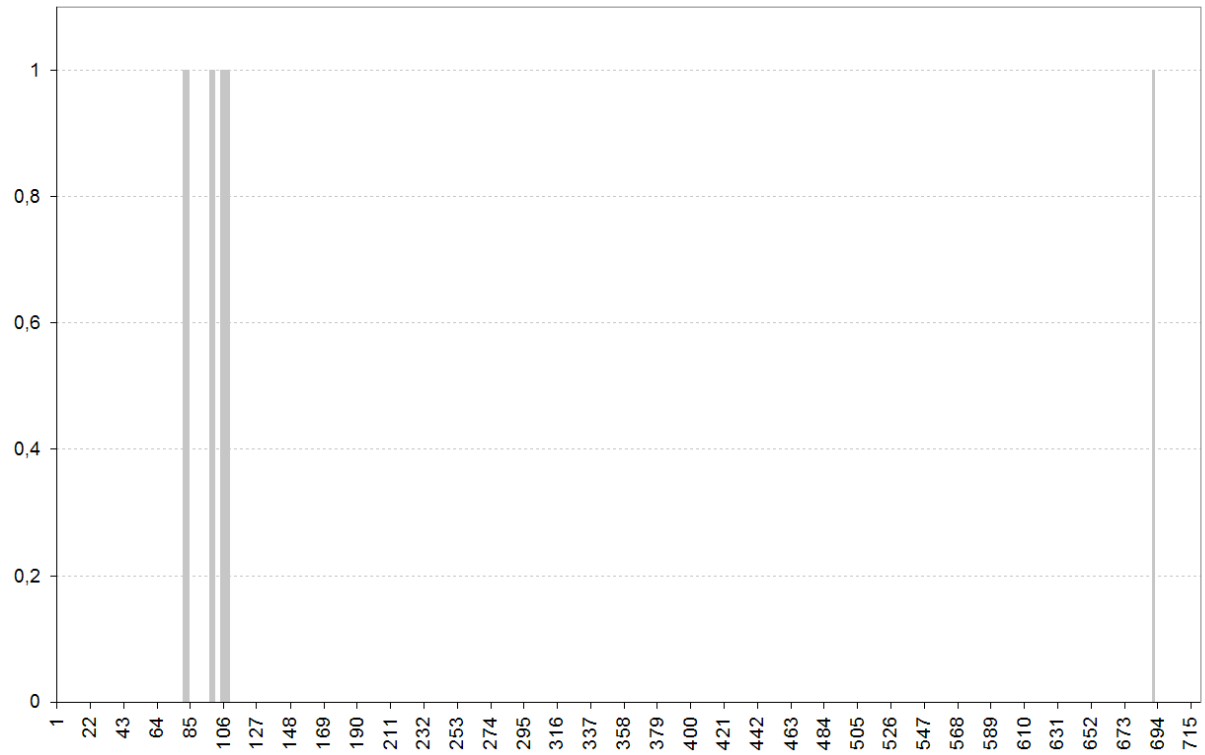

Figure 6: Jamming signalisation produced by the algorithms for the curves of figure 5 according to the conditions (2.1).

3 Results

Figures 2 and 6 show the jamming signalisation for one reflectivity image of the Montancy radar, which has a great regularity in jamming observation every day. Figure 7 shows an example of daily statistics of signalisation for four radars of the French radar network, and for the reflectivity images produced for the ODYSSEY data hub and compositing Centre, which produces OPERA radar composites. As every day 288 radar images are produced, these graphs indicate both the azimuths jammed and the frequency of the jamming for each day.

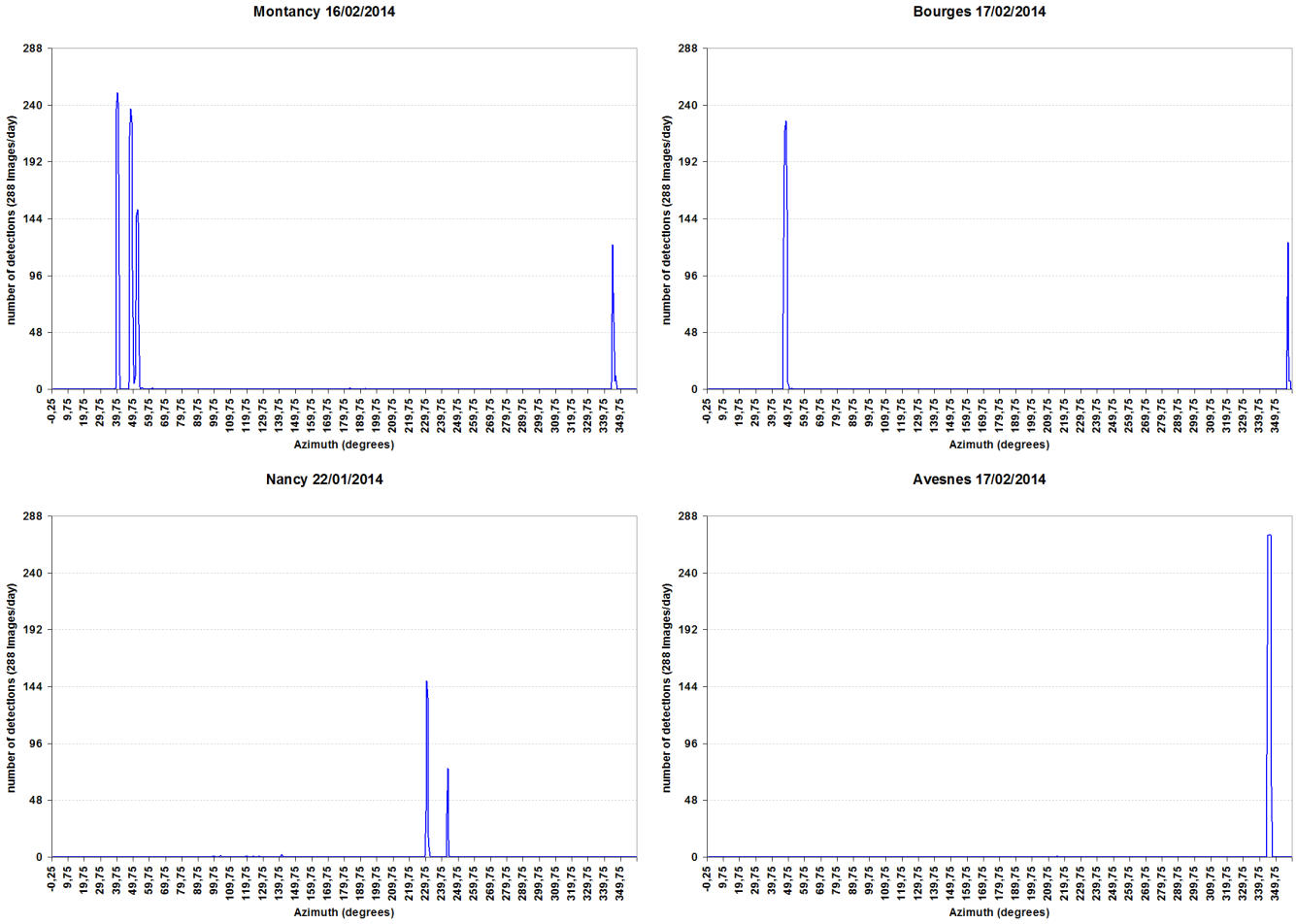

Figure 7: Number of daily jamming signalisations by azimuth for reflectivity images at lowest elevation of four radars of the French radar network. 288 images being produced by day for each radar parameter, these pictures show the frequency of jamming signalisation.

Producing performance criterions is not easy, because it may be difficult to define objectively the limit indicating when an image is jammed or not, and even more for each azimuth of this image. Furthermore, the jamming detection could be more or less easy depending on the radar or the rainy activity.

Table 1 and 2 present the result of an attempt to validate our jamming signalisations: for 12 radars of the French network, and for each radar for one day noticed as presenting jamming, we have visualised all the 1316 polar images signalled jammed, and all the other 1798 images for which no detection have been produced. For each image, it has been noticed:

- For table 1: if the image really shows an impact of jamming (even very lightly) or not, without taking into account in detail the number and position of azimuths considered jammed.
- For table 2: the number of azimuths really jammed, the number of false detection, and the number of azimuth jammed (even very lightly) not detected.

The values in table 1 indicate for jammed images a probability of detection (POD) and a critical success index (CSI) above 87%, and a probability of false detection (POFD) or a false alarm rate (FAR) below 0.7%. The values in table 2 indicate for each jammed azimuth a probability of detection (POD) and a critical success index (CSI) equal to 81%, and a false alarm rate (FAR) of 0. 5%. We can observe that the wrong signalisations of jammed images or azimuths are very few. The lack of detection is often due to very discontinuous signatures of first type, so corresponding to weak effect on the radar images quality. An other significant cause is the covering of jamming signature by rainy areas.

Table 1: Validation of the images signalled jammed for 12 radars of the French network (one day/radar, 3114 images).

		Detected Y	Detected N	
Observed	Y	1307	182	POD = 87.8% CSI = 87.2%
	N	9	1616	POFD = 0.6% FAR = 0.7%

Table 2: Validation of the 2206 azimuths signalled jammed for 12 radars of the French network (one day/radar, 3114 images).

		Detected Y	Detected N	
Observed	Y	2195	510	POD = 81.1% CSI = 80.8%
	N	11	/	POFD = / FAR = 0.5%

4 Conclusion

The signalisation of the first type of signature, concerning isolated rays, appears to be very effective except when this signature is very weak and discontinuous. In consequence, these detections have been used in some applications to filtered the radar rays concerned. The signalisation effectiveness of the second and third type of signatures depends on the thresholds used: the lower the threshold values are, the more sensitive the detection is, but the risk of false detections increases. The major difficulty is to exactly identify the angular size of the jammed sector. It is the purpose of the indicators analysis presented section 2.2, and the result is always a compromise: with the thresholds values presented in this communication, false detection rate is very acceptable, but the border of the jammed sectors could be not exactly identified. This is a limitation to the possibilities of image correction, not to the signalisation of jammed directions.

An other limitation inherent to the method, is that the geometric signatures can be used only in part of the image without rainfall, clear-air echoes or ground clutter. But this not seems to be a major limitation. An advantage of the geometric signatures use, is that the method is weakly sensitive to the radar calibration, and can be used for different radar parameters. So this method may constitute a complement or an alternative to others approaches.

We have tested these algorithms on images of reflectivity factor Z and on rain rate images, for two polar resolutions, i.e 720 *az* x 256 *bins* (range-resolution = 1 km) and 720 *az* x 1066 *bins* (range-resolution = 0.24 km), with the same choice of threshold values. The first type of signature detection also has been used on polar rain rate images with 360 *az* x 340 *bins* (range-resolution = 0.75 km). The results appear sufficient to signal the major observed jamming to the official Agency in charge of identifying the sources and of verifying the respect of the regulation concerning the authorisation of frequency use.